



CHALMERS

Chalmers Publication Library

The Circular Eleven Antenna: A New Decade-Bandwidth Feed for Reflector Antennas With High Aperture Efficiency

This document has been downloaded from Chalmers Publication Library (CPL). It is the author's version of a work that was accepted for publication in:

Ieee Transactions on Antennas and Propagation (ISSN: 0018-926X)

Citation for the published paper:

Yin, J. ; Yang, J. ; Pantaleev, M. (2013) "The Circular Eleven Antenna: A New Decade-Bandwidth Feed for Reflector Antennas With High Aperture Efficiency". Ieee Transactions on Antennas and Propagation, vol. 61(8), pp. 3976-3984.

<http://dx.doi.org/10.1109/tap.2013.2263275>

Downloaded from: <http://publications.lib.chalmers.se/publication/183018>

Notice: Changes introduced as a result of publishing processes such as copy-editing and formatting may not be reflected in this document. For a definitive version of this work, please refer to the published source. Please note that access to the published version might require a subscription.

Chalmers Publication Library (CPL) offers the possibility of retrieving research publications produced at Chalmers University of Technology. It covers all types of publications: articles, dissertations, licentiate theses, masters theses, conference papers, reports etc. Since 2006 it is the official tool for Chalmers official publication statistics. To ensure that Chalmers research results are disseminated as widely as possible, an Open Access Policy has been adopted. The CPL service is administrated and maintained by Chalmers Library.

(article starts on next page)

The Circular Eleven Antenna: A New Decade-bandwidth Feed for Reflector Antennas with High Aperture Efficiency

Jungang Yin, *Member, IEEE*, Jian Yang, *Senior Member, IEEE*, Miroslav Pantaleev, Leif Helldner

Abstract—Future ultra-wideband (UWB) radio telescopes require UWB feeds for reflector antennas, and many new UWB feed technologies have gained substantial progress to satisfy the tough specifications for future radio telescope projects, such as the square kilometer array (SKA). It has been noticed that, different from traditional narrow-band horn feeds, all UWB feeds are non-BOR (Body of Revolution) antennas. Therefore, BOR₁ efficiency becomes an important characterization for the modern UWB feed technologies. We present a novel circular Eleven feed, constructed of “circularly” curved folded dipoles printed on flat circuit boards, in order to have high BOR₁ efficiency at a low manufacture cost. The Genetic Algorithm (GA) optimization scheme has been applied to the design for achieving a low reflection coefficient. Simulated and measured results show that the circular Eleven feed has a reflection coefficient below -6 dB over 1.6–14 GHz and below -10 dB over 78% of the band, and an aperture efficiency higher than 60% over 1–10 GHz and 50% up to 14 GHz.

Index Terms—Eleven feed, BOR₁ efficiency, aperture efficiency, reflector antenna.

I. INTRODUCTION

LARGE decade-bandwidth reflector antennas are required in the next-generation radio telescopes, such as the 1–10GHz mid-band dish array of the SKA (Square Kilometer Array) project [1] and the 2–14GHz VLBI2010 (Very Long Baseline Interferometry 2010) project [2].

Several reflector feed technologies for decade-bandwidth radio telescopes are under development nowadays, such as the Eleven feed, the quadridge horn [3], the improved quadruple-ridged flared horn [4], the sinuous feed [5] and the quasi self-complementary antenna [6]. The main drawback of the quadridge horn as a feed for reflectors is that its beamwidth and phase center location vary with frequency, which leads to a low aperture efficiency; see the comparison of the radiation performance between the Eleven feed and the quadridge horn in [7]. The improved quadruple-ridged flared horn has much more constant beamwidth compared to the original quadridge horn but the phase center still varies with frequency. Both the sinuous feed and the quasi self-complementary antenna are

non-planer wideband log-periodic dual polarization antennas. The polarization angle of the two antennas varies with frequency and no hardware has yet been realized above 4 GHz.

The Eleven feed, featured as a low-profile ultra-wideband (UWB) antenna with a constant beamwidth and a fixed phase center location, has during the past years been developed at Chalmers University of Technology. It is referred to as the Eleven feed because its basic geometry consists of two parallel folded dipoles spaced half-wavelength apart above a ground plane, and it can have more than a decade bandwidth with 11 dBi directivity by extending the basic configuration logarithmically. It has been shown that the Eleven feed is well suitable for prime-fed reflectors in radio telescopes [8]–[13], and recent study shows that the Eleven feed is also suitable for offset Gregorian reflector system [14], [15]. In addition, the multi-port Eleven antenna has been studied for its versatility, such as for use in monopulse tracking systems [16] and UWB MIMO systems [17], [18].

It has been noticed that, different from the traditional narrow-band horn feeds, the geometries of all UWB and decade bandwidth feeds, including the above mentioned, are of non-BOR (Body of Revolution). Therefore, one important measure of the performance of these feeds is the so-called BOR₁ efficiency [19], [20] which characterizes how rotationally symmetric the radiation field function is.

In order to improve the BOR₁ efficiency of the Eleven feed, it is natural to make the folded dipoles, the radiation elements of the feed, more rotationally symmetric. It was reported in [21] that a flat circular single-folded dipole pair Eleven antenna had a higher BOR₁ efficiency, compared to the straight folded dipole pair one. However, it is very difficult to cascade scaled flat circular folded dipoles mechanically to achieve wideband performance.

In this paper, we propose a new circular Eleven feed, where the four petals of the circular folded dipole array are made on four pieces of flat printed circuit boards. A preliminary test-of-concept study on a 2–5GHz circular Eleven feed showed that the BOR₁ efficiency of the feed was improved [22]. A brief report on the current work over 1–14 GHz was presented in [23] with only simulation results, while in this paper a detailed description on the design with both simulations and measurements are presented.

The rest of this paper is organized as follows. In Sect. II, we describe the concept and the procedure of modeling the configuration of the circular Eleven feed, and a new method to compensate the effect of the non-logarithmically-scaled thick-

J. Yin was with the Dept. of Electronics and Telecommunications at Norwegian University of Science and Technology (NTNU), Trondheim, Norway, and now is with the Dept. of Electronics at Hunan University (HNU), Changsha, China. e-mail: jg_yin@hnu.edu.cn

J. Yang, M. Pantaleev and L. Helldner are respectively with the Dept. of Signals and Systems (Antenna Group) and the Dept. of Earth and Space Sciences (Onsala Space Observatory), Chalmers University of Technology, Gothenburg, Sweden.

Manuscript received 22 May, 2012.

ness of the substrate plate. In Sect. III, the genetic algorithm (GA) optimization is applied to a 7–14GHz model, and the optimized 7–14GHz feed is then extended directly to the 1–14GHz model. In Sect. IV, mechanical design and manufacture considerations are described. Comparison and discussion on simulated and measured performance are presented in Sect. V.

II. MODELING PROCEDURES IN CST

A. Reason for Circular Eleven Feed

The φ -variation of the far-field function of an antenna can always be expanded in a Fourier series, because φ is periodic with a period of 2π :

$$\mathbf{G}(\theta, \varphi) = \sum_{n=0}^{\infty} \{ [A_n(\theta)\sin(n\varphi) + B_n(\theta)\cos(n\varphi)]\hat{\theta} + [C_n(\theta)\cos(n\varphi) + D_n(\theta)\sin(n\varphi)]\hat{\varphi} \}. \quad (1)$$

It is known that only $n = 1$ component (referred to as BOR₁ component) in the Fourier series of the far-field function of a feed contributes to the directivity of the reflector antenna [19], [24], while all other $n \neq 1$ components cause sidelobes. Therefore, a high BOR₁ efficiency (the power in BOR₁ component relative to the total radiated power) is critical for achieving a high aperture efficiency and low sidelobes in feed design.

One way for a feed to achieve a high BOR₁ efficiency is to make its geometry more rotationally symmetric. As mentioned in Introduction, the one-pair flat circular Eleven feed has a higher BOR₁ efficiency than the straight one does [21]. However, it is very difficult to cascade such flat circular folded dipoles with a constant tilted angle relative to the ground plane, in order to have a wideband performance. To overcome this difficulty, a new circular Eleven feed configuration is proposed and described as follows.

B. Circularly Curved Folded Dipole Strips

Due to the symmetry, we model first only half of one petal of the circular Eleven feed, and then complete the four petals of the feed by mirroring the structure with respect to the two symmetry planes, x - z and y - z planes, in CST; see Fig. 1. The antenna petals are made on a printed circuit board with a 0.07-mm thick copper clad layer and a 0.381-mm thick Rogers TMM3 plate [25].

First, a right-angle triangular metal plate of 0.07-mm thick copper clad, with one cathetus lying in x - z plane, is tilted with an angle α_0 relative to x - y plane, as shown in Fig. 1(a). The apex point of the lower face of the metal plate is located at the origin of the coordinate system.

Then, a series of auxiliary cylinders of different diameters with its axis aligned in the z -axis are created. The basic idea of constructing the circular Eleven feed is to use these cylinders to intersect the tilted metal plate. After removing the intersections from the metal plate, the folded dipole strips are built, which look circular in the top view along the z -axis. In other words, the tilted folded dipoles have circular projections on the x - y plane, but actually are not exactly circular on

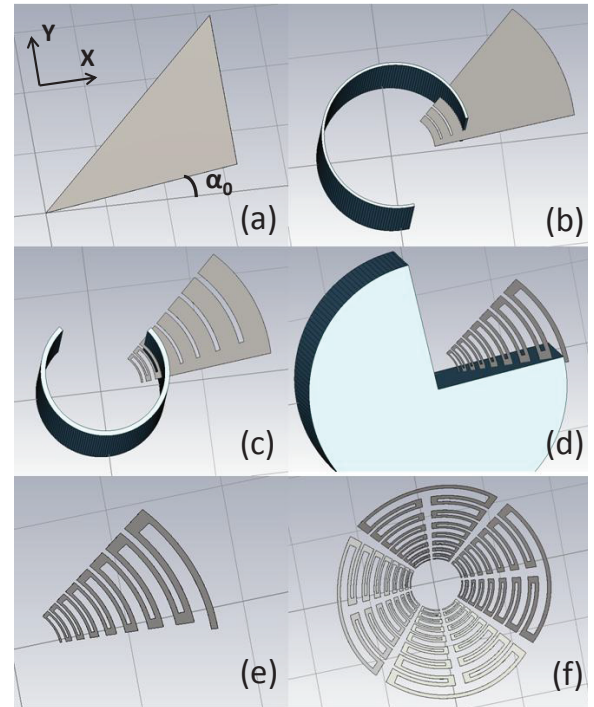


Fig. 1. CST modeling procedure of the metal strips of the circular folded dipole array for antenna petals, depicted briefly through subfigures (a) to (f).

the metal plate. We refer to these quasi-circular strips as the circular folded dipoles.

Thirdly, the innermost and the outermost ends of the triangular plate are trimmed by two auxiliary cylinders. Fig. 1 (b) shows how to use an auxiliary cylinder to make a circular inter-gap between adjacent folded dipoles, while in Fig. 1 (c) the making of a circular inner-gap between the arms of a folded dipole is illustrated. The central-gap between the two symmetric arms of the folded dipole is trimmed by an auxiliary cylinder, shown in Fig. 1 (d).

The TMM3 plate of a 0.381-mm thickness is then modeled below the dipole strips, with an apex angle of α_1 , shown in Fig. 2.

C. Antenna Geometry Parameters

The antenna geometry of the circular Eleven feed is composed of 4 cascaded log-periodic folded dipole arrays – the antenna petals.

The first folded dipole in the antenna petal is determined by the following parameters: the radius r_1 of an auxiliary cylinder to make the inner curvature, w_1 to determine the width of the folded dipole arms, s_1 to define the outer curvature by $r_1 + s_1$, and the four angles α_0 , α_1 , α_2 and α_3 . Please refer to Fig. 2 for the detailed definitions of these parameters. Note that these parameters are the measures of the projections of the folded dipole on x - y plane, which makes the modeling in CST very easy.

The length of the first folded dipole L_1 can be determined

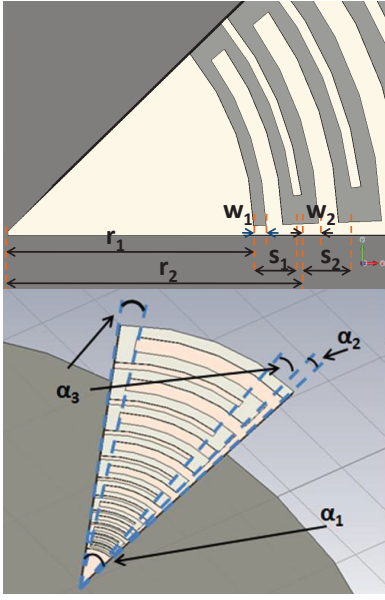


Fig. 2. Parameters that define the projection of antenna petal in $x-y$ plane, which therefore define the geometry of the petal.

TABLE I
ANTENNA GEOMETRY PARAMETERS WHERE $\lambda_{\text{geo1}}=15$ (MM)

Parameters	Initial Value	Parameters	Initial Value
$r_1/\lambda_{\text{geo1}}$	0.25	$s_1/\lambda_{\text{geo1}}$	0.05
$w_1/\lambda_{\text{geo1}}$	0.015	k	1.2
α_0	33.0°	α_1	42.0°
α_2	2.0°	α_3	4.0°

by

$$\frac{L_1}{\lambda_{\text{geo1}}} = \left(\frac{r_1}{\lambda_{\text{geo1}}} + \frac{s_1}{2\lambda_{\text{geo1}}} \right) \cdot \int_{-\alpha_1}^{\alpha_1} \sqrt{1 + \tan^2 \alpha_0 \sin^2 \varphi} d\varphi. \quad (2)$$

The derivation of this expression can be found in the appendix. The rest dipoles are determined by

$$\begin{aligned} r_n &= r_1 \cdot k^{n-1}, w_n = w_1 \cdot k^{n-1}, \\ s_n &= s_1 \cdot k^{n-1}, n = 2, \dots, N \end{aligned} \quad (3)$$

and the same four angles α_0 , α_1 , α_2 and α_3 , where k is the scaling factor of the log-periodic array. Then, the length of dipole n is

$$L_n = L_1 \cdot k^{n-1}, n = 2, \dots, N \quad (4)$$

D. Adjusted Scaling Factor Method

The wideband performance of the Eleven feed is obtained by cascading the log-periodically scaled elements. A PCB (printed circuit board) plate is employed to make the antenna petal in this work, and its copper sheet is very thin, $70 \mu\text{m}$. We can assume that the copper sheet is infinite thin so that the dipole stripes are purely log-periodically scaled. However, the substrate plate has to be thick enough to have the mechanical stability. Although the thickness of a substrate board can be changed with a log-periodic scale (for example by milling out

part of the substrate), it is very expensive to do so. In order to keep the manufacture cost low, we use a standard PCB plate with a constant thickness, i.e., 0.381-mm TMM3 plate in this work. Then, all dimensions of the antenna petal, except for the thickness of the PCB plate, are log-periodically scaled.

In order to compensate for the effect of this non log-periodically scaled substrate thickness, we introduce a so-called adjusted scaling factor method, where the scaling factor K_n for dipole n is scaled by a linearly adjusted factor q_n as

$$\begin{aligned} K_n &= k^{n-1} q_n, \\ q_n &= x + \frac{1-x}{(N-1)}(n-1), \\ 0.8 &\leq x \leq 0.95, \\ 1 &\leq n \leq N. \end{aligned} \quad (5)$$

where x is determined by the optimization procedure on the 7-14GHz model, and then adjusted a bit by try-and-error method for an optimal result when the 7-14GHz model is extended to the 1-14GHz feed. $x = 0.85$ is finally obtained in this work.

Eq. (5) implies that the maximum dimension shrinking by the adjusted factor happens on the innermost folded dipole, while there is no adjustment ($q_N = 1$) on the outermost dipole. The reason for doing so is that the substrate is the thickest in terms of the wavelength at the operation frequency of the innermost dipole (therefore strongest effect) and the thinnest in terms of the wavelength of the operation frequency of the outermost dipole.

It should be noted that the adjusted scaling factors are only applied to arm widths and lengths of folded dipoles in the cascaded array, i.e., w_i and L_i . The separation between pairs of folded dipoles, defined by r_i , should be half wavelength in free space in order to reduce the cross polarization level [8]. Then, (3) can be re-written as

$$\begin{aligned} r_n &= r_1 \cdot k^{n-1}, w_n = w_1 \cdot k^{n-1} q_n, \\ s_n &= s_1 \cdot k^{n-1}, L_n = L_1 \cdot k^{n-1} q_n. \end{aligned} \quad (6)$$

Note that now since L_n has been adjusted by q_n from its log-periodic scaled value, we should use (2) to calculate the different value of α_{1n} for each dipole in order to model the antenna in CST, where L_n cannot be used directly for the modeling. The α_{1n} values are obtained by solving (2) numerically via a matlab program.

III. OPTIMIZATION

The optimization model for the circular Eleven feed includes the four antenna petals, as shown in Fig. 3, in order to take into account the mutual coupling's effect from the orthogonal polarized petals. This, plus the curve geometry of the circular Eleven feed, makes it not suitable to apply the so-called partial array method presented in [11] for optimization. Therefore, we first optimized the geometry of a small circular Eleven antenna covering 7–14 GHz, and then extended this geometry directly to cover 1–14 GHz.

A. 7–14GHz Model

The model of the 7–14GHz circular Eleven feed with dual linear polarizations in CST is presented in Fig. 3,

which is defined by 9 parameters (Table I and x in (5)), as discussed in the previous section. For convenience, all dimensional parameters of each dipole are defined in terms of its geometrical wavelength λ_{geo} which is the wavelength of the operating frequency of the dipole [9]. The smallest geometrical wavelength $\lambda_{\text{geo}1}$, determining the dimensions of the first dipole, should be smaller than the wavelength of the lowest frequency in the operating band. Concerning the 7–14GHz model, $\lambda_{\text{geo}1}$ is set as 15 mm, corresponding to 20 GHz.

The value of $L_1/\lambda_{\text{geo}1}$ should be about 0.5. Plus with that $r_1/\lambda_{\text{geo}1}$ should be 0.25 in order to have a low cross polar level, we can set other parameters by (6) as middle values for the optimization; see Table I.

A discrete port with port impedance of 300Ω is placed across the feeding gap of the innermost dipole strips on the petal in the $x > 0$ region. Due to the symmetry of the geometry, the x - z plane is set as an electric symmetry plane, whereas the y - z plane is set as a magnetic symmetry plane, in the CST model. The transient solver of CST (based on integral time-domain method) is used with the number of hexahedral meshes in the order of several millions, where the setup of 50 meshes per wavelength and the smallest mesh size of 0.05 mm is used. It takes about 1 hour for one simulation on a workstation (Intel Core 2 Quad CPU @ 3.00 GHz, 8 GB RAM).

An in-house GA optimizer, implemented in MATLAB with calling CST to run the simulations, is used to optimize the geometry for the best reflection coefficient performance. Genetic algorithm (GA) has emerged during the past two decades as a practical optimization and search method in a variety of areas, such as electromagnetics, microelectronics, economic strategy planning, music generation, machine learning, etc [26]. Its stochastic nature makes it less prone to converge to a weak local optimum than deterministic optimization methods [27].

In our GA, a population of 200 individuals is created randomly in the first generation within a predefined range for the parameters, with the middle values shown in Table I. These individuals are checked, subject to some geometrical constraints in order to ensure the manufacturability. Then, the evolution repeats in generations based on the fitness values of the individuals. The fitness value of an individual is assigned by its lowest return loss (equivalent to the highest reflection coefficient) over the band. The fittest (with the highest fitness value) 10 individuals are selected as an elite group. Through crossover in the elite group, a pair of individuals as parents produce a pair of children who inherit exchanged or recombined chromosomes from both parents. For the rest of the generation, the selection mechanism (the higher the fitness value of an individual, the higher its chance to be selected) picks up individuals to pass their genes to the next generation. Through the 5% possibility of mutation, random alteration of the chromosomes of individuals can be caused. This evolution procedure is repeated until the geometries of the fittest individual in generations have converged. It is observed that 5 generations are sufficient for the solution achieves the convergence.

The results of the optimized geometric parameters are listed

TABLE II
OPTIMIZED ANTENNA GEOMETRY PARAMETERS WHERE $\lambda_{\text{geo}1}=15$ (MM)

Parameters	Optimized Value	Parameters	Optimized Value
$r_1/\lambda_{\text{geo}1}$	0.3091	$s_1/\lambda_{\text{geo}1}$	0.0493
$w_1/\lambda_{\text{geo}1}$	0.0115	k	1.2016
α_0	30.9520°	α_1	41.7531°
α_2	2.9262°	α_3	4.0936°

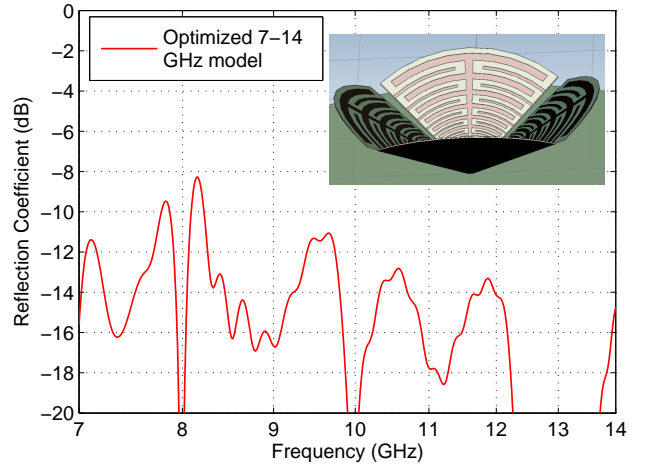


Fig. 3. The CST-simulated reflection coefficient of the optimized 7-14GHz Eleven model with input port impedance of 300Ω .

in Table II. Fig. 3 shows the simulated reflection coefficient of the optimized 7-14GHz Eleven model with the input port impedance of 300Ω . It can be observed that after the GA optimization, the reflection coefficient is below -10 dB over 7–14 GHz except for only two small spikes.

B. Full Antenna Model

Based on the optimized 7–14GHz model, the Eleven antenna over the full frequency range of 1–14 GHz is obtained by extending the 8-dipole geometry to a 17-dipole one using the same geometrical parameters. In fact, the innermost dipole operates at 20 GHz ($\lambda_{\text{geo}1} = 15$ mm) and the outermost dipole does at 1.06 GHz ($k = 1.2016$ after optimization). Considering the dielectric substrate boards, the outermost dipole can work at 1 GHz. Note that all dimensions are scaled except for the thicknesses of the dielectric substrates and the copper clay.

Compared in Fig. 4 are the reflection coefficients of the circular Eleven model (antenna petals only, without a center feeding circuit) with and without using the adjusted scaling method. With the adjusted scaling, the matching at high frequencies, especially above 12 GHz, is greatly improved; in the meanwhile, the matching at low frequencies, especially below 3 GHz, does not differ much between the two methods. It can be also observed that the direct extension of the 8-dipole array (7–14GHz model) to 17-dipole array (1–14GHz model) results in a reflection coefficient at -8dB level over 1–14 GHz, 2 dB worse than the 7–14GHz model.

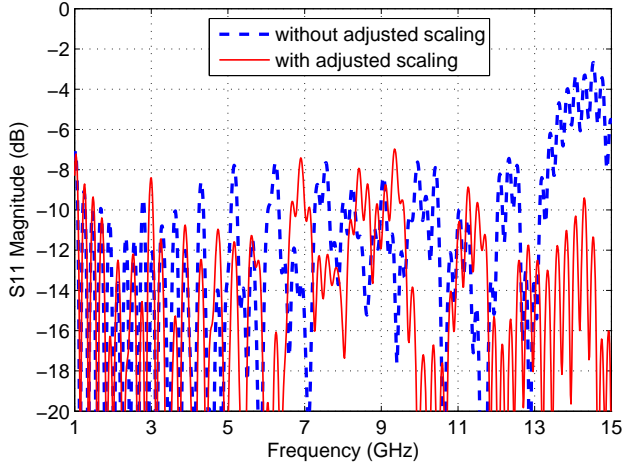


Fig. 4. CST-simulated S_{11} parameters of the circular Eleven antenna, with or without the adjusted scaling; in both cases, the antenna is fed by a $300\ \Omega$ discrete port without using a center puck.

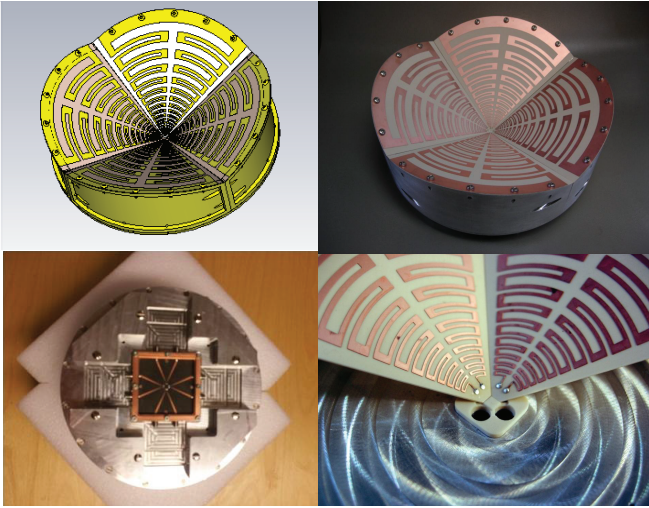


Fig. 5. The circular Eleven antenna with dual linear polarization, consisting of 17 folded dipoles on each petal. The diameter and the height of the feed are 210 mm and 65 mm, respectively. The antenna petals and the center puck on rear side are connected by twin lines that go through the ground plane via holes: (left-up) simulation model; (right-up) prototype; (left-down) center puck on rear side; (right-down) detailed center puck on front side.

C. 8-Port Center Puck

The 8-port feeding center puck (descrambling board) used in this work is shown in Fig. 5 (left-down). The main difference between this feeding center puck and the one in [13] is that the diameter of the twin lines through the ground plane via holes (Fig. 5 right-down) is reduced from 0.20 to 0.10 mm in order to match the port impedance of $300\ \Omega$, instead of the previous $200\ \Omega$. The center puck transforms the $300\ \Omega$ balanced twin-lines to the $50\ \Omega$ unbalanced coaxes with the help of linearly tapered microstrips.

Fig. 6 shows the simulated reflection coefficient of the 8 port feeding board, with a satisfactory performance over 1.6–14 GHz.

Then, the full model of 1–14GHz feed with the 8 port feeding board, shown in Fig. 5 left-up), was simulated by the

CST transient solver. The setup of 20 meshes per wavelength and the smallest mesh size of 0.05 mm is used. The total mesh number is in the order of several tens of millions, and the computation time for one simulation becomes about 20 hours on our server (Intel Xeon CPU @ 2.40 GHz, 8 processors, 72 GB RAM). Due to the large size of the geometry of the full model of the feed, we can not carry out any optimization on the whole feed.

IV. MECHANICAL DESIGN AND MANUFACTURE CONSIDERATIONS

Based on our experience of mechanical and cryogenic designs in the previous Eleven feed projects [13], [28], microstrip laminated circuit boards, with good thermal and mechanical properties for cryogenic operation, are used for both the antenna petals and center feeding circuit.

The main concerning factors to select the dielectric substrate are the low permittivity and matched expansion coefficients between the substrate and the copper, in order to minimize the deformation when the feed is cooled down to cryogenic temperatures. The TMM3 material from Rogers [25] is chosen as it satisfies the requirements well. To increase the thermal conductivity for a better antenna petal cooling, the copper cladding of $70\ \mu\text{m}$ is used.

The RF design requires the dielectric thickness of 0.381 mm. A careful modeling of the temperature distribution and the mechanical deformation on such thin TMM3 substrate has been set up and analyzed by using the software ANSYS [29]. Fig. 7 shows the simulated geometrical deformation of the circular Eleven feed when it is cooled down to 20 K. The results convince us that the selected substrate has a good performance, with little deformation and excellent mechanical stiffness at cryogenic temperature.

The mechanical deformation with cooling of outer side supporting walls has impact on the stress of the antenna petals. In order to minimize this stress, the deformations with the cooling should be matched between the outer walls and the antenna petals. We have performed the simulations of these deformations at 20 K: the radial deformation of the TMM3 petal, the aluminum walls and the copper walls are 0.48 mm, 0.45 mm and 0.41 mm, respectively. Therefore, the aluminum walls were selected in the design.

V. SIMULATED AND MEASURED RESULTS

The manufactured prototype of the circular feed, 210 mm in diameter and 65 mm in height, is shown in Fig. 5 (right-up). Note that all the measurements were carried out at room temperatures.

Both the simulated and the measured reflection coefficients are presented in Fig. 8. As we can see, the measured S_{11} magnitude is below $-6\ \text{dB}$ over the band of 1.6–14 GHz, and below $-10\ \text{dB}$ over 78% of 1.6–14 GHz. It is observed that there is a discrepancy between the simulated and the measured results. The reason for this, we believe, is that the mesh size in our model is not small enough to have an accurate modeling because of the limitation of the memory space of our server when the center puck circuit is included. The general mesh

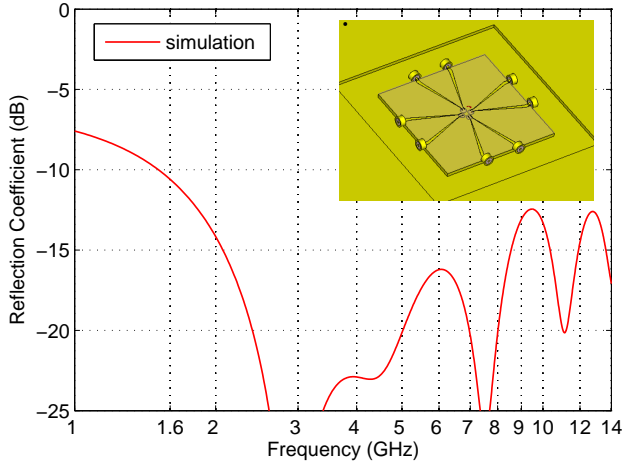


Fig. 6. Simulated reflection coefficients of the 8-port feeding center puck only.

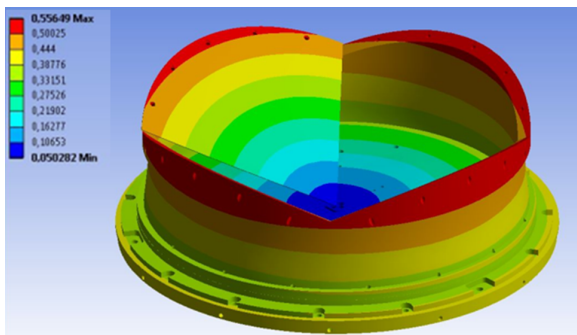


Fig. 7. Simulated geometrical deformations of the Eleven feed when it is at the cryogenic temperature of 20K.

size is set in the model as about 1.1 mm (20 mesh lines per wavelength at 14 GHz) and the smallest mesh size as 0.05 mm. The center puck circuit and the first dipoles are very tiny in dimension. For example, the diameter of the twin-line is 0.1 mm and only two meshes for the line. In addition, just beside the line, the mesh size jumps to 1.1 mm, which cannot take into account all effects of such thin twin-lines. We also find that due to such tiny geometry, some meshes are fulfilled by wrong materials automatically by CST (we cannot change them manually), such as TMM3 dielectric meshes are modeled by Copper, which leads to a significant discrepancy between the model and the real antenna for this tiny scale geometry. This explains that the discrepancy between the simulation and the measurement is more considerable at high frequencies due to the mesh size not small enough in general, and at low frequencies due to the model not accurate enough by the meshes. On the other hand, though we can model the feed more accurately with smaller meshes, the large simulation time prohibits us to run optimization on the whole feed geometry. We are working now on a new modeling-based optimization scheme, and upgrading our computer server. We believe that the reflection coefficient performance can be further improved by using the new optimization method and more powerful computers.

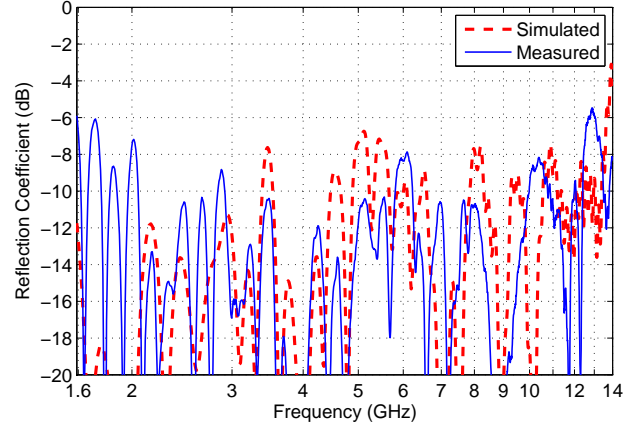


Fig. 8. Simulated and measured reflection coefficients of the circular Eleven feed prototype, including the 8-port feeding center puck.

Exhibited in Fig. 9 are the measured co- and cross-polar patterns of the total and BOR₁-component radiation patterns at 15 frequencies in the diagonal plane ($\varphi = 45^\circ$). It can be found that the cross-polar levels of the total field and the BOR₁ field are -10 dB and almost -20 dB below the maximum co-polar values over 1–14 GHz, respectively.

The aperture efficiency of a prime-focus reflector with a subtended angle of $2 \times 60^\circ$ fed by the circular Eleven feed is calculated based on both the simulated and the measured feed radiation patterns, as a sum of factorized sub-efficiencies, and presented in Fig. 10. As a reference, we reprint the calculated efficiencies based on measured radiation function of the previous 2–13GHz straight Eleven feed in [13] in Fig. 11. Note that the center and strut blockage loss is neglected in all e_{ap} calculations.

Very good agreement between the simulation and the measurement for the present circular Eleven feed is observed, which indicates that CST can predict the radiation performance of the whole feed well with the setup we used. The aperture efficiency is higher than 60% over 1–10 GHz and 50% up to 14 GHz, which is a significant improvement, especially below 2.2 GHz and above 13 GHz, compared to the previous 2–13GHz straight Eleven feed [13]. Note that the circular Eleven feed has a similar size to that of the previous one (present circular feed: diameter of 210 mm and height of 65 mm; previous straight feed: diameter of 200 mm and height of 62 mm).

The radiation efficiency of the prototype, a measure of its ohmic losses, was measured in a Bluetest reverberation chamber [30]. The simulation model of the feed is done in CST, as shown in Fig. 5 at the left-up corner. In the model, the annealed copper ($\sigma = 5.8 \times 10^7$ S/m) is used for all metal parts; the printed circuit boards used for the antenna petals and the center puck circuit are modeled on the substrate of Rogers TMM3 ($\epsilon_r = 3.27$, $\mu_r = 1$, $\tan\delta = 0.002$). All ohmic losses are therefore implemented in this model. The measured data are obtained by using a rigorous calibration method presented in [31].

The measured and the simulated data are presented in Fig. 12. It can be observed that the agreement between them is

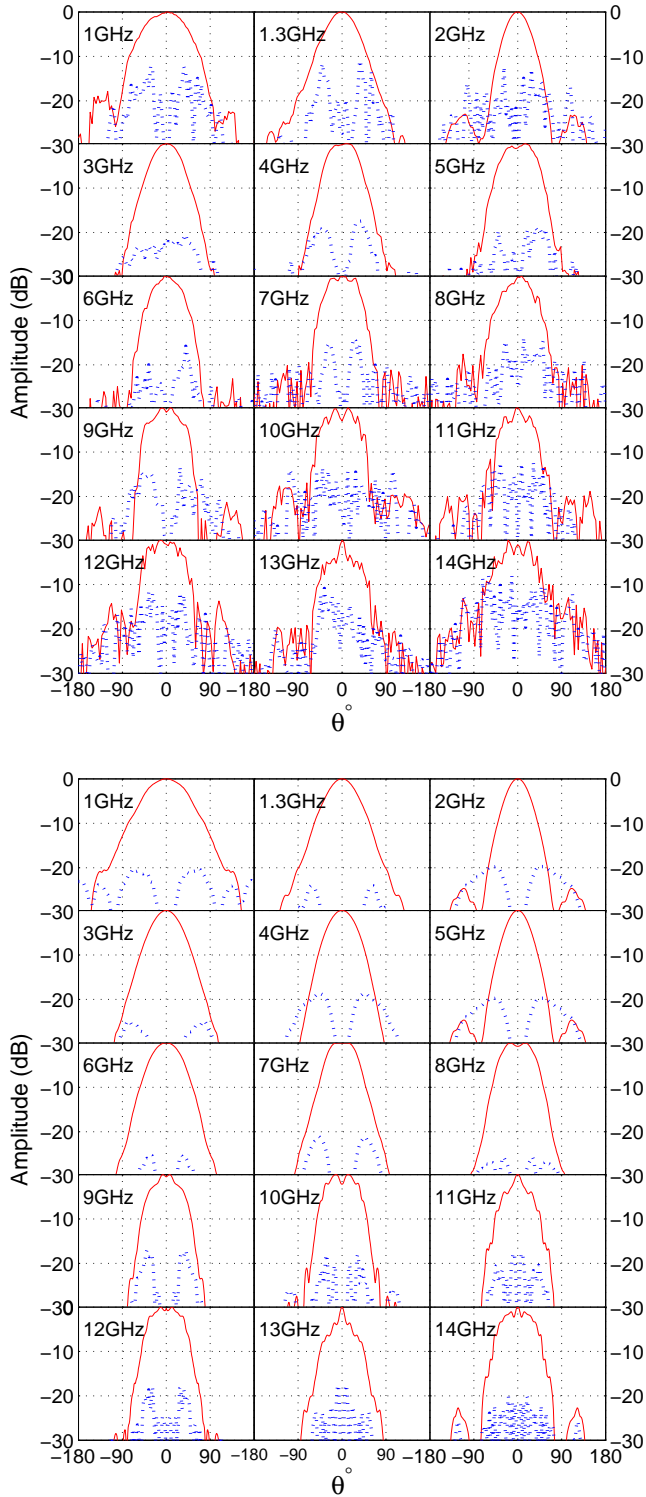


Fig. 9. Measured co- and cross-polar patterns of the total (upper) and BOR_1 component (lower) radiation field at 15 frequencies in $\varphi = 45^\circ$ plane.

good, considering that the measurement uncertainty in the reverberation chamber is 0.5 dB [32]. The fluctuation of the measured curve is caused by the limited number of the cavity modes in the reverberation chamber [32]. The overall radiation efficiency over the band is about -0.2 dB, corresponding to

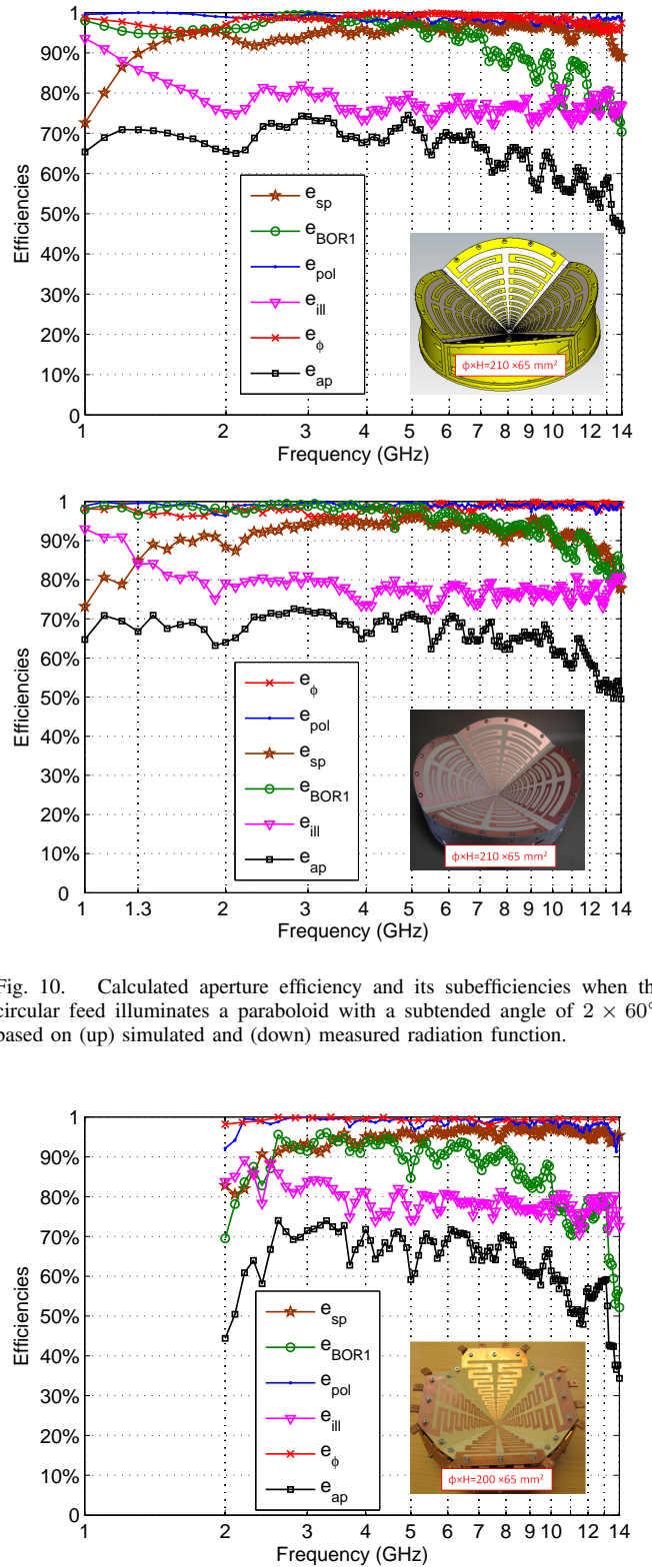


Fig. 10. Calculated aperture efficiency and its subefficiencies when the circular feed illuminates a paraboloid with a subtended angle of $2 \times 60^\circ$, based on (up) simulated and (down) measured radiation function.

Fig. 11. Calculated aperture efficiency of the previous 2-13GHz straight Eleven feed in [13] based on measured radiation function, as a reference to the present circular Eleven feed.

1.4 K increase for the antenna noise temperature when the feed is cooled down to 20 K inside a cryostat. Note that the measurement is done only up to 8 GHz due to the limitation

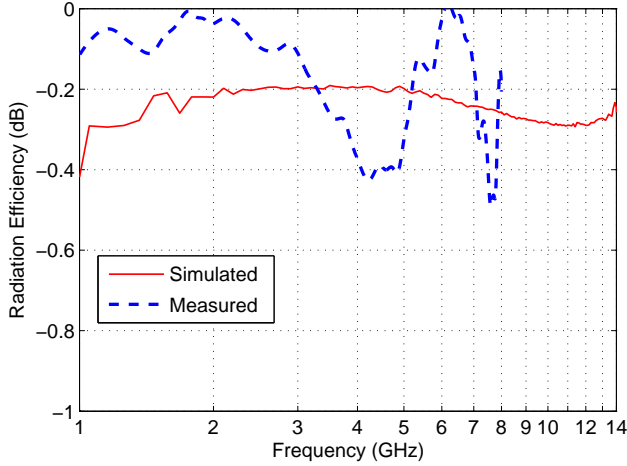


Fig. 12. Simulated and measured radiation efficiency of the feed including the 8-port center puck feeding circuit.

of the Bluetest chamber at the moment, and we are working on increasing the operating frequency of the Bluetest Chamber up to 16 GHz.

VI. CONCLUSION

We presented the design and development of the compact circular Eleven feed. An elaborate simulation model is built in CST and the new adjusted scaling method is introduced for compensating the effect of the thickness of substrate on antenna performance. Genetic algorithm optimization scheme is applied to a 7–14GHz model and then extended directly to a full model covering 1–14 GHz. A prototype is manufactured and tested. Confirmed by the good agreement between the simulations and the measurements, the aperture efficiency of a prime-focus reflector with the $2 \times 60^\circ$ subtended angle fed by the circular Eleven feed has achieved to above 60% over 1–10 GHz and above 50 % up to 14 GHz. This is a significant improvement on the aperture efficiency from the previous Eleven feeds. The reflection coefficient is below -6 dB over 1.6–14 GHz, and can be improved further down. We believe that the circular Eleven feed will find lots of applications in different wideband systems, such as ultra-wideband radio astronomy and multi-wideband satellite communications.

The circular Eleven feed is protected by a pending patent.

ACKNOWLEDGEMENT

The author Jungang Yin would like to thank Terje Mathiesen (with Dept. of Electronics and Telecommunications, NTNU) for his technical support on the pre-manufacture work.

This work was supported in part by The Swedish Foundation for Strategic Research (SSF) within the Strategic Research Center Charmant.

APPENDIX

The first circular folded dipole, of a cylindrical superficial arc, is formed by the intersection of a cylinder with a radius of $r_1 + 0.5s_1$ and a plane defined by:

$$z = \tan \alpha_0 \cdot x. \quad (7)$$

The projection of the cylindrical superficial arc L on x - y plane is a circular arc S (ranged by angle $\pm\alpha_1$), and the differential of L can be approximated by using plane trigonometry:

$$\begin{aligned} dL &= \sqrt{(dS)^2 + (dz)^2} \\ &= \sqrt{(dx)^2 + (dy)^2 + (dz)^2} \\ &= \sqrt{[1 + \tan^2 \alpha_0](dx)^2 + (dy)^2} \end{aligned} \quad (8)$$

L can be integrated along the circular arc S :

$$L = \int_S \sqrt{[1 + \tan^2 \alpha_0](dx)^2 + (dy)^2} \quad (9)$$

And S can be parameterized by angle φ ,

$$\begin{aligned} x &= (r_1 + 0.5s_1) \cdot \cos \varphi \\ y &= (r_1 + 0.5s_1) \cdot \sin \varphi \\ -\alpha_1 &\leq \varphi \leq \alpha_1 \end{aligned} \quad (10)$$

Inserting (10) into (9), we finally obtain

$$\begin{aligned} L &= (r_1 + 0.5s_1) \\ &\cdot \int_{-\alpha_1}^{\alpha_1} \sqrt{[1 + \tan^2 \alpha_0](\sin \varphi d\varphi)^2 + (\cos \varphi d\varphi)^2} \\ &= (r_1 + 0.5s_1) \cdot \int_{-\alpha_1}^{\alpha_1} \sqrt{1 + \tan^2 \alpha_0 \sin^2 \varphi} d\varphi \end{aligned} \quad (11)$$

REFERENCES

- [1] P. Hall, "The square kilometre array: An international engineering perspective," *The Square Kilometre Array: An Engineering Perspective*, pp. 5–16, 2005.
- [2] A. Niell, A. Whitney, B. Petrachenko, W. Schluter, N. Vandenberg, H. Hase, Y. Koyama, C. Ma, H. Schuh, and G. Tuccari, "VLBI2010: current and future requirements for geodetic VLBI systems," *Report of Working Group*, vol. 3, 2005.
- [3] V. Rodriguez, "An open-boundary quad-ridged guide horn antenna for use as a source in antenna pattern measurement anechoic chamber," *IEEE Antennas Propog. Mag.*, vol. 48, no. 2, pp. 157–160, Apr. 2006.
- [4] A. Akgiray, S. Weinreb, and W. Imbriale, "Design and measurements of dual-polarized wideband constant-beamwidth quadruple-ridged flared horn," in *2011 IEEE AP-S International Symp. on Antennas Propag.* Spokane, Washington: IEEE, 3-8 July 2011, pp. 1135–1138.
- [5] R. Gawande and R. Bradley, "Towards an ultra wideband low noise active sinuous feed for next generation radio telescopes," *IEEE Trans. Antennas Propag.*, no. 99, pp. 1945–1953, June 2011.
- [6] G. Cortes-Medellin, "Non-planar quasi-self-complementary ultra-wideband feed antenna," *IEEE Trans. Antennas Propog.*, vol. 59, no. 6, pp. 1935–1944, June 2011.
- [7] J. Yang, S. Pivnenko, and P.-S. Kildal, "Comparison of two decade-bandwidth feeds for reflector antennas: the eleven antenna and quadridge horn," in *2010 Proceedings of the Fourth European Conference on Antennas and Propagation (EuCAP2010)*.
- [8] R. Olsson, P.-S. Kildal, and S. Weinreb, "The Eleven antenna: a compact low-profile decade bandwidth dual polarized feed for reflector antennas," *IEEE Trans. on Antennas Propag.*, vol. 54, no. 2, pp. 368–375, Feb. 2006.
- [9] J. Yang, X. Chen, N. Wadefalk, and P.-S. Kildal, "Design and realization of a linearly polarized eleven feed for 1–10 GHz," *IEEE Antennas Wireless Propagat. Lett.*, vol. 8, pp. 64–68, 2009.
- [10] J. Yang, D. Nyberg, and J. Yin, "Impedance matrix of a folded dipole pair under eleven configuration," *IET Microwaves Antennas Propagat.*, vol. 4, no. 6, pp. 697–703, June 2010.
- [11] J. Yang and P.-S. Kildal, "Optimization of reflection coefficient of large log-periodic array by computing only a small part of it," *IEEE Trans. Antennas Propag.*, vol. 59, no. 6, pp. 1790–1797, June 2011.
- [12] J. Yang, "On conditions for constant radiation characteristics for log-periodic array antennas," *IEEE Trans. Antennas Propag.*, vol. 58, no. 5, pp. 1521–1526, May 2010.

- [13] J. Yang, M. Pantaleev, P.-S. Kildal, B. Klein, Y. Karadikar, L. Helldner, N. Wade-falk, and C. Beaudoin, "Cryogenic 2–13 GHz Eleven feed for reflector antennas in future wideband radio telescopes," *IEEE Trans. Antennas Propag.*, vol. 59, no. 6, pp. 1918–1934, June 2011.
- [14] J. Yang, M. Pantaleev, T. Ekebrand, P.-S. Kildal, H. Raza, J. Yin, J. Jonsson, L. Helldner, A. Emrich, and B. Klein, "Development of the cryogenic 2–14 GHz Eleven feed system for VLBI2010," in *6th Eur. Conf. on Antennas Propag. (EuCAP2012)*, Prague, 26–30 March 2012.
- [15] M. Pantaleev, J. Yin, M. Ivashina, and J. Conway, "Eleven feed project: development of broadband cryogenic frontend prototype for the SKA," SPO report, Tech. Rep., 2012.
- [16] J. Yin, J. A. Aas, J. Yang, and P.-S. Kildal, "Monopulse tracking performance of multi-port Eleven antenna for use in terminals for satellite communications." The 2nd Eur. Conference on Antennas and Propagation (EuCAP 2007), Edinburgh, 11 - 16 November 2007.
- [17] X. Chen, P.-S. Kildal, J. Carlsson, and J. Yang, "Comparison of ergodic capacities from wideband mimo antenna measurements in reverberation chamber and anechoic chamber," *IEEE Antennas Wireless Propag. Lett.*, vol. 10, pp. 446–449, 2011.
- [18] J. Yang, S. Pivnenko, T. Laitinen, J. Carlsson, and X. Chen, "Measurements of diversity gain and radiation efficiency of the Eleven antenna by using different measurement techniques." Barcelona: 4th European Conference on Antennas and Propagation, (EuCAP 2010), April 2010.
- [19] P.-S. Kildal and Z. Sipus, "Classification of rotationally symmetric antennas as types BOR₀ and BOR₁," *IEEE Antennas Propag. Mag.*, Dec. 1995.
- [20] P.-S. Kildal, "Factorization of the feed efficiency of paraboloids and cassegrain antennas," *IEEE Trans on Antennas and Propag.*, vol. 33, no. 8, pp. 903–908, Feb. 1985.
- [21] A. Yasin, J. Yang, and T. Ostling, "A compact dual-band feed for reflector antennas based on choke horn and circular eleven antenna," *IEEE Trans. Antennas Propag.*, vol. 57, no. 10, pp. 3300–3302, 2009.
- [22] J. Yin and J. Yang, "A 2–5 GHz circular Eleven antenna with improved BOR1 efficiency," in *2011 IEEE International Symposium on Antennas and Propagation (APSURSI)*. IEEE, Spokane, 2011, pp. 1247–1250.
- [23] J. Yin, J. Yang, M. Pantaleev, and L. Helldner, "A circular Eleven feed with significantly improved aperture efficiency over 1.3–14 GHz," in *6th Eur. Conf. on Antennas Propag. (EuCAP2012)*, Prague, 26–30 March 2012.
- [24] W. V. T. Rusch and P. D. Potter, *Analysis of Reflector Antennas*. New York: Academic, 1970.
- [25] <http://www.rogerscorp.com/acm/products/14/TMM-Thermoset-Microwave-Laminates-Thermoset-ceramic-loaded-plastic.aspx>.
- [26] M. Srinivas and L. M. Patnaik, "Genetic algorithms: A survey," *IEEE Computer*, vol. 27, no. 6, pp. 17–26, June 1994.
- [27] D. S. Weile and E. Michielssen, "Genetic algorithm optimization applied to electromagnetics," *IEEE Trans. Antennas Propag.*, vol. 45, no. 7, pp. 343–353, March 1997.
- [28] J. Yang, M. Pantaleev, P.-S. Kildal, and L. Helldner, "Design of compact dual-polarized 1.2–10 GHz Eleven feed for decade bandwidth radio telescopes," *IEEE Trans. Antennas Propag.*, vol. 60, no. 5, pp. 2210–2218, May, 2012.
- [29] <http://www.ansys.com/>.
- [30] Bluetest AB; <http://www.bluetest.se>.
- [31] H. Raza, J. Yang, and A. Hussain, "Measurement of radiation efficiency of multiport antennas with feeding network corrections," *IEEE Antennas and Wireless Propagation Letters*, vol. 11, pp. 89–92, 2012.
- [32] P.-S. Kildal, X. Chen, C. Orlenius, M. Franzén, and C. L. Patane, "Characterization of reverberation chambers for OTA measurements of wireless devices: Physical formulations of channel matrix and new uncertainty formula," *IEEE Transactions on Antennas and Propagation*, vol. 60, no. 8, pp. 3875–3891, 2012.



Jungang Yin (M'11) received the B.Sc. degree from Beijing Institute of Technology, Beijing, China, in 2000, and the M.Sc. degree from Royal Institute of Technology (KTH), Stockholm, Sweden, in 2005, both in electrical engineering. In 2011, he achieved his Ph.D. degree in electronics and telecommunications from Norwegian University of Science and Technology (NTNU), Trondheim, Norway. He has during the recent years been working on the Eleven feed system for next generation radiotelescope technology in collaboration with the Antenna Group and Onsala Space Observatory at Chalmers University of Technology, Gothenburg, Sweden. His research interests include, among others, design of antennas/RF front-end systems and signal processing.



Jian Yang (M'02-SM'10) received the B.S. degree from the Nanjing University of Science and Technology, Nanjing, China, in 1982, and the M.S. degree from the Nanjing Research Center of Electronic Engineering, Nanjing, China, in 1985, both in electrical engineering, and the Swedish Licentiate and Ph.D. degrees from the Chalmers University of Technology, Gothenburg, Sweden, in 1998 and 2001, respectively. From 1985 to 1996, he was with the Nanjing Research Institute of Electronics Technology, Nanjing, China, as a Senior Engineer. From 1999 to 2005, he was with the Department of Electromagnetics, Chalmers University of Technology as a Research Engineer. During 2005 and 2006, he was with COMHAT AB as a Senior Engineer. From 2006 to 2010, he was an Assistant Professor, and since 2010, he has been Associate Professor, at the Department of Signals and Systems, Chalmers University of Technology. His research interests include 60–120 GHz antennas, THz antennas, ultra-wideband antennas and UWB feeds for reflector antennas, UWB radar systems, UWB antennas in near-field sensing applications, hat-fed antennas, reflector antennas, radome design, and computational electromagnetics.



Miroslav Pantaleev received the M.S. degree in electrical engineering from the Technical University of Sofia, Sofia, Bulgaria, in 1995, and the M.S. and Ph.D. degrees from the Chalmers University of Technology, Gothenburg, Sweden, in 2000 and 2006, respectively. During his doctoral studies, he was involved in beam measurement characterization for HIFI Instrument of Herschel satellite and later in the design and tests of the HEB mixer for the APEX telescope. He is currently the Head of the Operation and Development Laboratory, Onsala Space Observatory, Onsala, Sweden, where he is responsible for design, integration, implementation, and testing of radio-astronomical equipment. His main areas of research are low noise cryogenic amplifiers and mixers, system integration of optical, cryogenic and mechanical components, and cryogenic techniques for laboratory applications.

Observatory, Onsala, Sweden, where he is responsible for design, integration, implementation, and testing of radio-astronomical equipment. His main areas of research are low noise cryogenic amplifiers and mixers, system integration of optical, cryogenic and mechanical components, and cryogenic techniques for laboratory applications.



Leif Helldner has been a Research Engineer in the Operation and Development Laboratory at Onsala Space Observatory since 1989. For more than twenty years he has been working with development, test and maintenance of front-end and back-end electronics for radio astronomy. He has excellent experience in design and test of RF, IF, automatization and digital electronics, mechanical and cryogenic systems for radio astronomy. He has been involved in developing hardware systems for SEST, APEX, ALMA and the Onsala telescopes and radiometers,

and was the project manager for the construction of a LOFAR station in Sweden. His interests are mechanical and cryogenic design, and international VLBI and LOFAR technical activities.